

## Photon-Initiated Homolysis of Peroxynitrous Acid

Manuel Sturzbecher-Höhne, Thomas Nauser, Reinhard Kissner, and Willem H. Koppenol\*

Institute of Inorganic Chemistry, Department of Chemistry and Applied Biosciences, ETH Zurich, 8093 Zurich, Switzerland

Received March 30, 2009

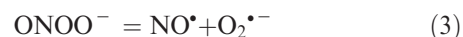
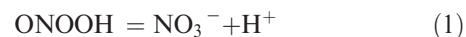
Laser flash photolysis of ONOOH at 355 nm and a pH of 4.0–5.5 causes homolysis of ONOOH nearly exclusively at the N–O bond rather than at the O–O bond ( $\text{HO}_2^\bullet/\text{HO}^\bullet > 25:1$ ). All of the  $\text{NO}^\bullet$  and  $\text{HO}_2^\bullet$  radicals formed by photolysis subsequently recombine with a rate constant of  $(1.2 \pm 0.2) \times 10^{10} \text{ M}^{-1} \text{ s}^{-1}$  via second-order kinetics, as demonstrated by the return of the UV/vis absorbance to initial levels. Excitation at 266 nm also yields  $\text{HO}_2^\bullet$  and  $\text{NO}^\bullet$ , but after recombination, the absorbance levels are lower than initial values, possibly because  $\text{HO}^\bullet$  produced by the photolysis of water reacts with ONOOH. When  $\text{NO}_3^-$ , the product of the ONOOH isomerization, is photolyzed, the  $\text{ONOO}^-$  formed is rapidly protonated with a second-order rate constant of  $(1.7 \pm 0.8) \times 10^{10} \text{ M}^{-1} \text{ s}^{-1}$ . The ONOOH decays to the starting material,  $\text{NO}_3^-$ , with a first-order rate constant of  $1.2 \text{ s}^{-1}$ . The quantum yield for the photon-initiated homolysis is 15% for both ONOOH and  $\text{ONOO}^-$ . We conclude that the ON–OOH and ON–OO<sup>−</sup> bond dissociation energies are similar.

### Introduction

Peroxynitrous acid, ONOOH,<sup>1</sup> a strong oxidant as well as a nitrating agent, may be formed in vivo<sup>2,3</sup> by the diffusion-limited reaction of  $\text{O}_2^{\bullet-}$  and the cellular messenger  $\text{NO}^\bullet$ ,  $k = (1.6 \pm 0.3) \times 10^{10} \text{ M}^{-1} \text{ s}^{-1}$ .<sup>4</sup> ONOOH and  $\text{ONOO}^-$  react with a variety of biomolecules<sup>5,6</sup> and are implicated in a variety of diseases and disorders, including atherosclerosis, inflammation, and neurodegenerative disorders.<sup>5,7</sup>

$\text{ONOO}^-$  is fairly stable in aqueous media at pH values above 10. In the protonated form, ONOOH decays to  $\text{NO}_3^-$

with a rate constant of  $1.2 \text{ s}^{-1}$  (reaction 1).<sup>8</sup> The  $\text{p}K_a$  of ONOOH is 6.5–6.8 (reaction 2), depending on the ionic strength of the solution.<sup>8</sup>



Homolysis of  $\text{ONOO}^-$  at the N–O bond (reaction 3) takes place with a rate constant of  $0.020 \pm 0.001 \text{ s}^{-1}$ .<sup>9</sup> From this rate constant and the known rate constant for reaction 3,  $(1.6 \pm 0.3) \times 10^{10} \text{ M}^{-1} \text{ s}^{-1}$ ,<sup>4</sup> we derived standard Gibbs energies of formation of  $\text{ONOO}^-$  ( $+68 \pm 1 \text{ kJ mol}^{-1}$ ) and ONOOH

\*To whom correspondence should be addressed. Phone: +41-44-632-2875. Fax +41-44-632-1090. E-mail: koppenol@inorg.chem.ethz.ch.

(1) Formulae, systematic names, and *trivial* names (in italics):  $\text{ONOO}^-$ , oxidoperoxidodinitrate(1−), *peroxynitrite*; ONOOH, (hydridodioxido)oxidonitrogen, *peroxynitrous acid*;  $\text{O}_2^{\bullet-}$ , dioxide(•1−), *superoxide*;  $\text{HO}_2^\bullet$ , hydridodioxxygen(•), *perhydroxyl radical* or *hydroperoxyl radical*;  $\text{O}_2$ , dioxygen;  $\text{O}^{\bullet-}$ , oxide(•1−);  $\text{NO}^\bullet$ , oxidonitrogen(•) or nitrogen monoxide, *nitric oxide*;  $\text{NO}_2^\bullet$ , dioxidonitrogen(•) or nitrogen dioxide, *pernitric oxide*;  $\text{N}_2\text{O}_4$ , tetraoxidodinitrogen, *nitrogen tetroxide*;  $\text{NO}_3^-$ , trioxidonitrate(1−), *nitrate*;  $\text{HO}^\bullet$ , hydridooxygen(•), *hydroxyl radical*;  $\text{Cl}_2^{\bullet-}$ , dichloride(•1−), *dichlorine radical anion*. Connelly, N. G.; Damhus, T.; Hartshorn, R. M.; Hutton, A. T. *Nomenclature of Inorganic Chemistry. IUPAC Recommendations 2005*; Royal Society of Chemistry: Cambridge, U.K., 2005.

(2) Beckman, J. S.; Beckman, T. W.; Chen, J.; Marshall, P. A.; Freeman, B. A. *Proc. Natl. Acad. Sci. U. S. A.* **1990**, *87*, 1620–1624.

(3) Beckman, J. S.; Koppenol, W. H. *Am. J. Physiol. Cell Physiol.* **1996**, *271*, C1424–C1437.

(4) Nauser, T.; Koppenol, W. H. *J. Phys. Chem. A* **2002**, *106*, 4084–4086.

(5) Alvarez, B.; Radi, R. *Amino Acids* **2003**, *25*, 295–311.

(6) Szabo, C.; Ischiropoulos, H.; Radi, R. *Nat. Rev. Drug Discovery* **2007**, *6*, 662–680.

(7) Pacher, P.; Beckman, J. S.; Liaudet, L. *Physiol. Rev.* **2007**, *87*, 315–424.

(8) Kissner, R.; Nauser, T.; Bugnon, P.; Lye, P. G.; Koppenol, W. H. *Chem. Res. Toxicol.* **1997**, *10*, 1285–1292.

(9) Sturzbecher, M.; Kissner, R.; Nauser, T.; Koppenol, W. H. *Inorg. Chem.* **2007**, *46*, 10655–10658.

(+31 ± 1 kJ mol<sup>-1</sup>), in excellent agreement with other published values.<sup>10–13</sup> We summarize the published thermodynamic values in Figure 1. The Gibbs energies of formation of ONOOH (+31 ± 1 kJ mol<sup>-1</sup>),<sup>10,12</sup> NO<sub>2</sub><sup>•</sup> (63 ± 1 kJ mol<sup>-1</sup>),<sup>14</sup> and HO<sup>•</sup> (26 ± 1 kJ mol<sup>-1</sup>)<sup>15,16</sup> and the published rate constant for reaction 4 (4.5 × 10<sup>9</sup> M<sup>-1</sup> s<sup>-1</sup>)<sup>17,18</sup> have been used to predict a rate of homolysis of ONOOH at the O–O bond (reaction 4) of 0.38 ± 0.25 s<sup>-1</sup>.<sup>10,11,19</sup> However, this approach is valid only when no branching of the reaction coordinate occurs, which is not the case here: the reaction of HO<sup>•</sup> with NO<sub>2</sub><sup>•</sup> yields two products, namely, ONOOH and NO<sub>3</sub><sup>-</sup>/H<sup>+</sup>.<sup>18</sup> Since we have searched for, but have been unable to find, evidence of significant levels of formation of HO<sup>•</sup> from ONOOH,<sup>20–24</sup> we attempted to stimulate reaction 4 by laser flash photolysis.

A pathway of homolysis of ONOOH, distinct from reaction 4, leads to the formation of NO<sup>•</sup> and HO<sub>2</sub><sup>•</sup> (reaction 5). The energies of these products of reaction lie 20 kJ mol<sup>-1</sup> above those of the products of reaction 4 (Figure 1): Δ<sub>r</sub>G<sup>o</sup>(NO<sup>•</sup>) = 102 ± 0.2 kJ mol<sup>-1</sup> is calculated from Δ<sub>f</sub>G<sup>o</sup>(NO<sup>•</sup>)<sub>g</sub> = +86.57 kJ mol<sup>-1</sup><sup>25</sup> and Henry's constant, 1.92 × 10<sup>-3</sup> M 0.100 MPa<sup>-1</sup><sup>26</sup> at 25 °C; Δ<sub>r</sub>G<sup>o</sup>(HO<sub>2</sub><sup>•</sup>) = 6.4 ± 1.0 kJ mol<sup>-1</sup> is based on E<sup>o</sup>(O<sub>2</sub>/O<sub>2</sub><sup>•-</sup>) = 350 ± 11 mV<sup>27</sup> and pK<sub>a,6</sub> = 4.8 ± 0.1 for HO<sub>2</sub><sup>•</sup>.<sup>28</sup> With k<sub>-5</sub> = 3.2 × 10<sup>9</sup> M<sup>-1</sup> s<sup>-1</sup><sup>29</sup> and the Gibbs energies of formation of ONOOH, NO<sup>•</sup>, and HO<sub>2</sub><sup>•</sup>, we calculate k<sub>5</sub> = (0.8 ± 1.0) × 10<sup>-4</sup> s<sup>-1</sup>, which is more than 4 orders of magnitude lower than k<sub>4</sub>.

We report here that NO<sup>•</sup> and HO<sub>2</sub><sup>•</sup>, but not NO<sub>2</sub><sup>•</sup> and HO<sup>•</sup>, are formed by the photolysis of ONOOH. The observed products recombine rapidly to form ONOOH.

## Materials and Methods

**Chemicals.** (Me<sub>4</sub>N)ONOO was prepared from NO<sup>•</sup> and (Me<sub>4</sub>N)O<sub>2</sub> according to the method of Bohle et al.<sup>30–32</sup>

- (10) Merényi, G.; Lind, J. *Chem. Res. Toxicol.* **1998**, *11*, 243–246.  
 (11) Goldstein, S.; Czapski, G.; Lind, J.; Merényi, G. *Chem. Res. Toxicol.* **2001**, *14*, 657–660.  
 (12) Merényi, G.; Lind, J.; Czapski, G.; Goldstein, S. *Inorg. Chem.* **2003**, *42*, 3796–3800.  
 (13) Lyman, S. V.; Poskrebyshev, G. A. *J. Phys. Chem. A* **2003**, *107*, 7991–7996.  
 (14) Stanbury, D. M. *Adv. Inorg. Chem.* **1989**, *33*, 69–138.  
 (15) Schwarz, H. A.; Dodson, R. W. *J. Phys. Chem.* **1984**, *88*, 3643–3647.  
 (16) Klänning, U. K.; Sehested, K.; Holcman, J. *J. Phys. Chem.* **1985**, *89*, 760–763.  
 (17) Logager, T.; Sehested, K. *J. Phys. Chem.* **1993**, *97*, 6664–6669.  
 (18) Merényi, G.; Lind, J.; Goldstein, S.; Czapski, G. *J. Phys. Chem. A* **1999**, *103*, 5685–5691.  
 (19) Lyman, S. V.; Khairutdinov, R. F.; Hurst, J. K. *Inorg. Chem.* **2003**, *42*, 5259–5266.  
 (20) Kissner, R.; Koppenol, W. H. *J. Am. Chem. Soc.* **2002**, *124*, 234–239.  
 (21) Maurer, P.; Thomas, C. F.; Kissner, R.; Rügger, H.; Greter, O.; Röthlisberger, U.; Koppenol, W. H. *J. Phys. Chem. A* **2003**, *107*, 1763–1769.  
 (22) Kissner, R.; Nauser, T.; Kurz, C.; Koppenol, W. H. *IUBMB Life* **2003**, *55*, 567–572.  
 (23) Kissner, R.; Thomas, C.; Hamsa, M. S. A.; van Eldik, R.; Koppenol, W. H. *J. Phys. Chem. A* **2003**, *107*, 11261–11263.  
 (24) Kurz, C.; Zeng, X.; Hannemann, S.; Kissner, R.; Koppenol, W. H. *J. Phys. Chem. A* **2005**, *109*, 965–969.  
 (25) Wagman, D. D.; Evans, W. H.; Parker, V. B.; Schumm, R. H.; Halow, I.; Bailey, S. M.; Churney, K. L.; Nuttall, R. L. *J. Phys. Chem. Ref. Data* **1982**, *11*(Suppl. 2), 37–38.  
 (26) Wilhelm, E.; Battino, R.; Wilcock, R. *J. Chem. Rev.* **1977**, *77*, 219–262.  
 (27) Wardman, P. *Free Radical Res. Commun.* **1991**, *14*, 57–67.  
 (28) Bielski, B. H. J.; Cabelli, D. E.; Arudi, R. L. *J. Phys. Chem. Ref. Data* **1985**, *14*, 1041–1100.  
 (29) Goldstein, S.; Czapski, G. *Free Radical Biol. Med.* **1995**, *19*, 505–510.  
 (30) Bohle, D. S.; Hansert, B.; Paulson, S. C.; Smith, B. D. *J. Am. Chem. Soc.* **1994**, *116*, 7423–7424.  
 (31) Bohle, D. S.; Glassbrenner, P. A.; Hansert, B. *Methods Enzymol.* **1996**, *269*, 302–311.  
 (32) Bohle, D. S.; Sagan, E. S. *Inorg. Synth.* **2004**, *34*, 36–42.

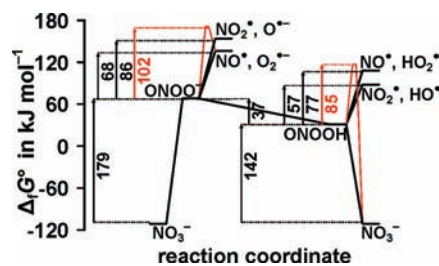


**Figure 1.** The reaction coordinate for the photolysis of NO<sub>3</sub><sup>-</sup> showing Gibbs energies of formation of ONOOH, ONOO<sup>-</sup>, and NO<sub>3</sub><sup>-</sup> and possible products of homolysis and experimentally determined activation energy barriers. Activation energies and the barriers for homolysis of ONOO<sup>-</sup> to NO<sup>•</sup> and O<sub>2</sub><sup>•-</sup> and isomerization of ONOOH to NO<sub>2</sub><sup>•</sup> and HO<sup>•</sup> are shown in red. Gibbs energies of reaction are shown in black.

All reagent gases were obtained from PanGas (Dagmersellen, CH). LiONOO was prepared as previously described.<sup>33</sup> All other chemicals were obtained at the highest purity available and used as received. A Millipore Milli-Q unit (Molsheim, F) was used to purify deionized water.

**Instrumentation.** UV/vis spectra were recorded with a double-beam Analytik Jena Specord 200 (Jena, D). Rapid mixing was achieved by the stopped-flow mixing unit from Applied Photophysics, SX 17MV (Leatherhead, Surrey, Great Britain), that was operated in the symmetric mixing mode interfaced to an Applied Photophysics LKS 50 instrument (Leatherhead, Surrey, Great Britain). The quartz cell was asymmetric with a 10 mm optical path length, a 2 mm laser path length, and a total volume of 0.08 cm<sup>3</sup>; measurements were performed at 25 °C, maintained with a thermostat. Optical changes were collected and stored on a WaveRunner 64Xi digital oscilloscope from Lecroy (Chestnut Ridge, NY). The bandwidth chosen for these experiments was 20 MHz, and the sampling rate was 200 MHz. The third (λ = 355 nm) or fourth (λ = 266 nm) harmonic of a Quantel Brilliant B Nd:YAG laser (Les Ulis Cedex, F) was used with a pulse duration of 6 ns and spot size of 9 mm. The laser energies were determined with a PRD-J peak-reading joulemeter from Gentec Inc. (Sainte-Foy, Quebec, Canada). The pH was measured with a Metrohm glass electrode (Herisau, Switzerland) interfaced with a 901 microprocessor analyzer from Orion Research, Inc. (Cambridge, MA).

**Methods. Photolysis of NO<sub>3</sub><sup>-</sup>.** Argon-saturated 1 M NO<sub>3</sub><sup>-</sup> solutions were excited at 266 nm at pH 2.9–4.4, and subsequent reactions were followed at 260 and 330 nm. Highly concentrated solutions of NO<sub>3</sub><sup>-</sup> were used because of the low absorbance of NO<sub>3</sub><sup>-</sup> at 266 nm (ε<sub>266</sub> = 1.5 M<sup>-1</sup> cm<sup>-1</sup>). ONOO (M = (Me<sub>4</sub>N)<sup>+</sup>, Li<sup>+</sup>) solutions were freshly prepared in 10 mM MOH (M = K<sup>+</sup>, Li<sup>+</sup>), kept in the dark on ice.

**Photolysis of ONOO<sup>-</sup>.** Argon-saturated solutions of ONOO<sup>-</sup> at ca. 2 mM in 10 mM MOH were mixed by stopped-flow techniques at 25 °C with either 20 mM H<sub>3</sub>PO<sub>4</sub> or 100 mM pivalate buffer as a proton source to final pH values of 2–5.5. After 5 ms of mixing, excitation of ONOOH was achieved with a laser pulse of 266 or 355 nm with energies of 10–140 mJ/pulse (266 nm) or

(33) Sturzbecher-Höhne, M.; Kissner, R.; Nauser, T.; Koppenol, W. H. *Chem. Res. Toxicol.* **2008**, *21*, 2257–2259.

**Table 1.** Molar Absorptivities of Relevant Species, Used to Calculate Yields and Spectra in Figures 3 and 5

	Excitation $\lambda$ (nm)		Observation $\lambda$ (nm)		
	266, $\epsilon$ ( $M^{-1}$ $cm^{-1}$ )	355, $\epsilon$ ( $M^{-1}$ $cm^{-1}$ )	260, $\epsilon$ ( $M^{-1}$ $cm^{-1}$ )	330, $\epsilon$ ( $M^{-1}$ $cm^{-1}$ )	400, $\epsilon$ ( $M^{-1}$ $cm^{-1}$ )
ONOOH <sup>8</sup>	450	70	500	80	8
ONOO <sup>-8</sup>	680	500	475	850	71
HO <sup>+45</sup>			480		
HO <sup>+46</sup>			430		
HO <sup>+47</sup>			454	135	30
HO <sub>2</sub> <sup>+28,35</sup>			540		
O <sub>2</sub> <sup>+28,35</sup>			1940		
NO <sup>*</sup>			> 10	> 10	> 10
NO <sub>2</sub> <sup>+48</sup>			270	150	200
N <sub>2</sub> O <sub>4</sub> <sup>36,49</sup>			750	300	

10–160 mJ/pulse (355 nm), and reactions were followed at 260, 330, and 400 nm. The pH was recorded after mixing. Transient absorbance changes at pH 4.8 were recorded by changing the wavelength settings of the monochromator in 5 nm increments from 235–300 nm. The concentration of HO<sup>\*</sup>, generated in photolysis experiments, was determined by mixing ONOO<sup>-</sup> in a 1:1 ratio with NaCl at different concentrations in 20 mM HCl before excitation with detection of the transient Cl<sub>2</sub><sup>•-</sup> at 340 nm ( $\epsilon_{340} = 8800 M^{-1} cm^{-1}$ <sup>34</sup>); NaCl solutions photolyzed in 10 mM HCl served as controls.

## Results

**Photolysis of NO<sub>3</sub><sup>-</sup>.** We investigated the photolysis of NO<sub>3</sub><sup>-</sup>, the product of isomerization of ONOOH, in the presence of the cations Li<sup>+</sup>, Na<sup>+</sup>, K<sup>+</sup>, Cs<sup>+</sup>, and (Me<sub>4</sub>N)<sup>+</sup>. We did not use RbNO<sub>3</sub>, because it is not sufficiently soluble in aqueous solution. All alkali metal salts of NO<sub>3</sub><sup>-</sup> behave similarly: during excitation at pH 2.9–4.4, an initial increase in absorbance at 330 nm is observed that is ascribed to the formation of ONOO<sup>-</sup>, followed by a rapid decay that is linearly dependent on the H<sup>+</sup> concentration and represents protonation of ONOO<sup>-</sup>. The protonation takes place with a second-order rate constant of  $(1.7 \pm 0.8) \times 10^{10} M^{-1} s^{-1}$  (data not shown). From the absorbance of the initial product and reported absorptivities for ONOO<sup>-</sup> at 260 nm ( $\epsilon = 500 M^{-1} cm^{-1}$ ) and 330 nm ( $\epsilon = 80 M^{-1} cm^{-1}$ )<sup>8</sup> (Table 1), we calculated that excitation at 266 nm with a laser energy of 100 mJ/pulse results in the formation of 10  $\mu M$  ONOOH. After the protonation step, we observe a first-order decay to initial absorbance levels at 260 nm with a rate constant of  $1.2 s^{-1}$ , which we assign to the isomerization of ONOOH to NO<sub>3</sub><sup>-</sup>/H<sup>+</sup>. The behavior of (Me<sub>4</sub>N)NO<sub>3</sub> was different from that of the alkali metal salts, with a slower increase in absorbance followed by only a single decay.

**Photolysis of ONOOH.** Laser flash photolysis experiments were performed with Li<sup>+</sup> as the counterion. LiONOO (1.76 mM) was rapidly mixed with an equal

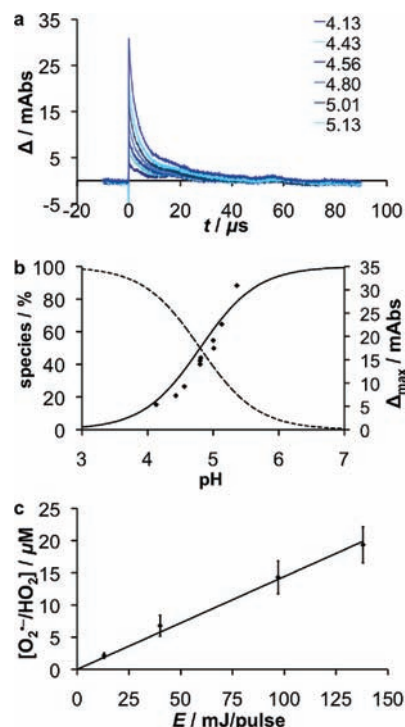


**Figure 2.** Photolysis (355 nm) of ONOOH, prepared by mixing 2.06 mM LiONOO in 10 mM LiOH, with a 0.1 M pivalate buffer, at pH 4.1–5.4 and 25 °C. (a) Absorbance increase at 260 nm upon irradiation and subsequent decay attributed to second-order recombination. The signal distortion at 58  $\mu s$  was also observed in the absence of ONOOH. (b) Absorbance at 260 nm (red data points) measured directly after irradiation (140 mJ/pulse), with the species distributions of HO<sub>2</sub><sup>\*</sup> (dashed line) and O<sub>2</sub><sup>•-</sup> (solid line) calculated on the basis of  $pK_a = 4.8$ . (c) Concentration of HO<sub>2</sub><sup>\*</sup>/O<sub>2</sub><sup>•-</sup>, based on absorbance at 260 nm, as a function of laser energy.

amount of 20 mM H<sub>3</sub>PO<sub>4</sub> (final pH 2.1) and irradiated with laser pulses at 355 nm. Only small changes in absorbance were detected: the highest laser energy used (142 mJ/pulse) resulted in an increase of 0.004 absorbance units at 260 nm relative to the preirradiation level. Importantly, the subsequent decay in absorbance to the preirradiation absorbance level obeys second-order kinetics and is complete after 50  $\mu s$ . The low signal-to-noise ratio obviated meaningful evaluation of the traces. We found larger absorbance changes at higher pH, and Figure 2a shows data collected in a 100 mM pivalate buffer at pH 4.1–5.4. The increase in absorbance at 260 nm as a function of pH approximates that expected for HO<sub>2</sub><sup>\*</sup>, the  $pK_a$  of which is 4.8 (Figure 2b).<sup>28</sup> When the irradiation energy is varied, a strictly linear correlation between the concentration of HO<sub>2</sub><sup>\*</sup>/O<sub>2</sub><sup>•-</sup> and laser energy is found (Figure 2c). Kinetics data obtained in additional experiments performed with (Me<sub>4</sub>N)ONOO were similar to those obtained with LiONOO.

We plotted the absorbance measured at 5 nm intervals between 235 and 300 nm after excitation (355 nm, 125 mJ/pulse) at pH 4.83 (after mixing) in Figure 3a. At pH 4.8, the concentrations of HO<sub>2</sub><sup>\*</sup> and O<sub>2</sub><sup>•-</sup> are the same, and we used molar absorptivities from the literature<sup>28,35</sup> to evaluate the concentrations and rate constants to generate the calculated mixed spectrum shown in Figure 3b. That

(34) Under acidic conditions, Cl<sup>-</sup> reacts quickly with HO<sup>\*</sup> to form ultimately the strongly absorbing Cl<sub>2</sub><sup>•-</sup>. This is shown in the reactions below. The yield of the transient Cl<sub>2</sub><sup>•-</sup> is dependent on the Cl<sup>-</sup> concentration and the laser energy. HO<sup>\*</sup> + Cl<sup>-</sup> = HOCl<sup>•-</sup>, HOCl<sup>•-</sup> + H<sup>+</sup> = H<sub>2</sub>O + Cl<sup>•</sup>, Cl<sup>•</sup> + Cl<sup>-</sup> = Cl<sub>2</sub><sup>•-</sup>. Jayson, G. G.; Parsons, B. J.; Swallow, A. J. *J. Chem. Soc., Faraday Trans. 1* **1973**, 69, 1597–1607.

(35) Bielski, B. H. J. *Photochem. Photobiol.* **1978**, 28, 645–649.

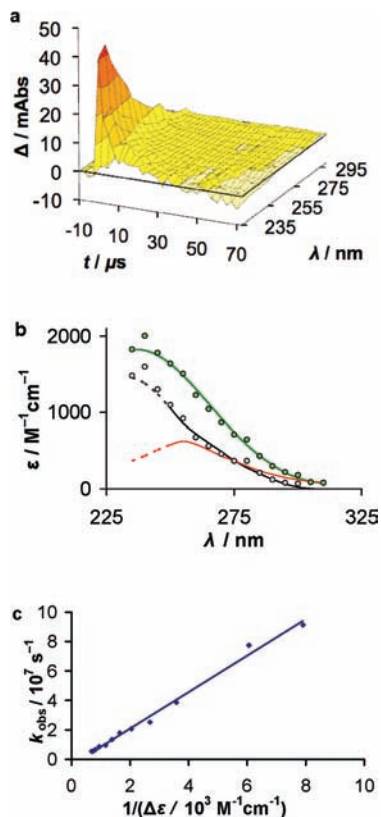


**Figure 3.** Spectral changes upon photolysis (355 nm, 125 mJ/pulse) of 1.1 mM (Me<sub>4</sub>N)ONOO at pH 4.8 and 25 °C, prepared from equal volumes of 2.2 mM (Me<sub>4</sub>N)ONOO in 10 mM KOH and a 0.1 M pivalate buffer. (a) Spectrum as a function of time after the pulse, showing apparent second-order decay to initial absorbance levels via recombination of HO<sub>2</sub><sup>•</sup>/O<sub>2</sub><sup>•-</sup> with NO<sup>•</sup>, yield of HO<sub>2</sub><sup>•</sup>/O<sub>2</sub><sup>•-</sup> > 25 μM. (b) Raw spectral data (gray circles) recorded 0.07 μs after photolysis of ONOOH at pH 4.8. Spectrum of HO<sub>2</sub><sup>•</sup>/O<sub>2</sub><sup>•-</sup> (green line) calculated for pH = pK<sub>a,6</sub> = 4.8;<sup>28,35</sup> experimental spectrum of ONOOH (red line), extrapolated to λ < 250 nm based on an assumed symmetric band; difference spectrum, Δε (gray line) = ε (HO<sub>2</sub><sup>•</sup>/O<sub>2</sub><sup>•-</sup>, green line) - ε (ONOOH, red line). Spectral data corrected for the bleaching of ONOOH (green points). Data points are derived from the data in a. Note that the measured absorptivities and, hence, the shape of the spectra are not dependent on the time elapsed after the flash over the range of 0.07–5 μs. The data fit a model for exclusive formation of NO<sup>•</sup> and HO<sub>2</sub><sup>•</sup> (reaction 5). (c) The observed rate constant as a function of the reciprocal effective molar absorptivity (the sum of the molar absorptivities of HO<sub>2</sub><sup>•</sup>, O<sub>2</sub><sup>•-</sup>, and ONOOH at 235–300 nm) at pH 4.8: a second-order rate constant of (1.2 ± 0.2) × 10<sup>10</sup> M<sup>-1</sup> s<sup>-1</sup> for the reaction of HO<sub>2</sub><sup>•</sup> and NO<sup>•</sup> to form ONOOH is determined from the slope of the line. Rate constants are derived from the data in a.

the absorbance maximum of the transient species lies near 240–245 nm is evidence for the formation of HO<sub>2</sub><sup>•</sup>/O<sub>2</sub><sup>•-</sup>, which indicates that irradiation causes homolysis of the N–O bond. The decay of the transient species is expected to correspond to the reaction of HO<sub>2</sub><sup>•</sup> with NO<sup>•</sup> to reform ONOOH, which should follow second-order kinetics. The concentration of HO<sub>2</sub><sup>•</sup>/O<sub>2</sub><sup>•-</sup> immediately following irradiation with a laser energy of 125 mJ/pulse is > 25 μM. The decay rates are plotted as a function of the reciprocal of the extinction coefficient in Figure 3c, from which we determine a second-order rate constant of (1.2 ± 0.2) × 10<sup>10</sup> M<sup>-1</sup> s<sup>-1</sup> for reaction 5.

(36) Hug, G. L. *Optical Spectra of Nonmetallic Inorganic Transient Species in Aqueous Solution*, NSRDS-NBS 69; National Bureau of Standards: Washington, DC, 1981.

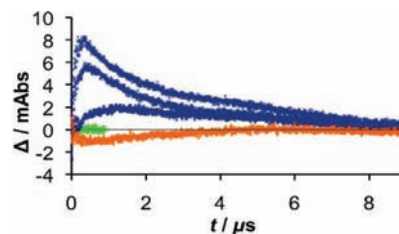


**Figure 4.** Trapping of HO<sup>•</sup>. Detection of Cl<sub>2</sub><sup>•-</sup> at 340 nm (ε = 8800 M<sup>-1</sup>cm<sup>-1</sup>) formed in the reaction of Cl<sup>-</sup> with HO<sup>•</sup> in acidic solution. Solutions of 1 mM ONOOH (pH 2.1) were irradiated (355 nm, 135 mJ/pulse) in the presence of 10 mM, 60 mM, and 110 mM chloride (blue traces). The yields of Cl<sub>2</sub><sup>•-</sup> increase with [Cl<sup>-</sup>] to a maximum of 0.9 μM. Control experiments: photolysis of 1.0 mM ONOOH in the absence of Cl<sup>-</sup>, orange trace, and photolysis of 10 mM Cl<sup>-</sup> in the absence of ONOOH, green trace.

To probe for the formation of NO<sub>2</sub><sup>•</sup>, we analyzed the kinetics of the reaction at 330 and 400 nm, where the absorptivity of NO<sub>2</sub><sup>•</sup> and its dimer N<sub>2</sub>O<sub>4</sub> is higher than that of ONOOH.<sup>8,36</sup> No change in absorbance was detected at 400 nm, but we observed a transient decrease in the absorbance at 330 nm that within 5 μs returned to the initial level (data not shown).

We also attempted to find evidence for the formation of HO<sup>•</sup> during the photolysis of ONOOH, via its reaction with Cl<sup>-</sup> under acidic conditions.<sup>34</sup> Solutions of NaCl at various concentrations at pH 2 (HCl) were mixed 1:1 with 2.03 mM ONOO<sup>-</sup> and irradiated. At the highest Cl<sup>-</sup> concentration (110 mM) and a laser energy of 135 mJ/pulse, the concentration of Cl<sub>2</sub><sup>•-</sup> generated from HO<sup>•</sup> is only 0.9 μM. In the absence of Cl<sup>-</sup>, the absorbance at 340 nm of a 1.01 mM ONOOH solution initially decreases, then returns to the initial level (Figure 4). In the absence of ONOOH, but with Cl<sup>-</sup> present, no absorbance changes after excitation at 355 nm were observed.

We also performed photolysis of ONOOH at 266 nm (100 mJ/pulse) at pH 4.83 (after mixing) and found corroborating evidence for the formation of HO<sub>2</sub><sup>•</sup> (Figure 5), followed by second-order decay. The concentration of HO<sub>2</sub><sup>•</sup>/O<sub>2</sub><sup>•-</sup> after irradiation is 125 μM, much higher than that found after excitation at 355 nm, as expected since the molar absorptivity of ONOOH at 266 nm (450 M<sup>-1</sup> cm<sup>-1</sup>) is much higher than at 355 nm, (70 M<sup>-1</sup> cm<sup>-1</sup>).<sup>8</sup> While photolysis at 355 nm is fully reversible, that at 266 nm is not: the absorbance at 235–310 nm is significantly lower at the end of the experiment, likely due to a fast reaction of ONOOH with HO<sup>•</sup> or H<sup>•</sup> and e<sub>aq</sub><sup>-</sup>, which originate from the two-photon excitation of H<sub>2</sub>O<sup>37,38</sup> and, to a minor degree, by HO<sup>•</sup> formed in reaction 4. By the irradiation of acidic Cl<sup>-</sup> solutions, we determined that HO<sup>•</sup> is formed in concentrations up to 5 μM.

When experiments were carried out over the wavelength range 235–300 nm, we observed for both excitation wavelengths that the rate constants increase with decreasing molar absorptivities of HO<sub>2</sub><sup>•</sup> and

(37) Reuther, A.; Lauberau, A.; Nikogosyan, D. N. *J. Phys. Chem.* **1996**, *100*, 16794–16800.

(38) Görner, H.; Nikogosyan, D. N. *J. Photochem. Photobiol. B: Biol.* **1997**, *39*, 84–89.

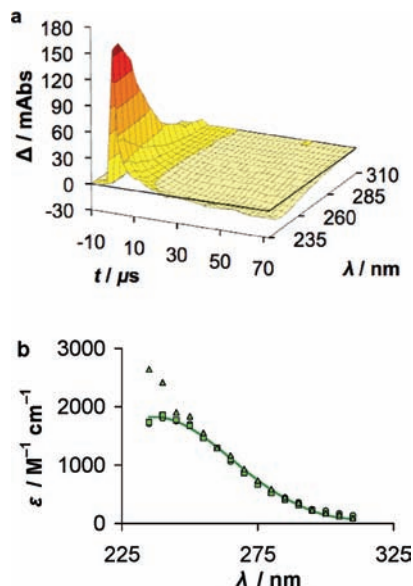


**Figure 5.** Spectral changes upon photolysis (266 nm, 100 mJ/pulse) of 1.1 mM (Me<sub>4</sub>N)ONOO at pH 4.8 and 25 °C, prepared from equal volumes of 2.2 mM (Me<sub>4</sub>N)ONOO in 10 mM KOH and a 0.1 M pivalate buffer. (a) Spectrum as a function of time after the pulse, showing apparent second-order decay via recombination of HO<sub>2</sub>•/O<sub>2</sub>•<sup>-</sup> with NO•, ca. 125 μM yield of HO<sub>2</sub>•/O<sub>2</sub>•<sup>-</sup>. In contrast to photolysis at 355 nm (Figure 3a), the absorbance of the reaction mixture decays to a level lower than the initial level. (b) Spectral data, corrected for the bleaching of ONOOH, recorded at 0.07 μs (green circles) and 5 μs (green triangles) after photolysis of ONOOH at pH 4.8 and calculated spectrum of HO<sub>2</sub>•/O<sub>2</sub>•<sup>-</sup> at pH 4.8 (green line), as in Figure 3b. Data points are derived from the data in a. In contrast to photolysis at 355 nm (Figure 3b), a systematic deviation from a model for exclusive formation of NO• and HO<sub>2</sub>• (reaction 5) is observed at λ > 300 nm for 0.07 μs time points (circles) and at λ < 250 nm for 5 μs points (triangles).

O<sub>2</sub>•<sup>-</sup> (for excitation at 355 nm, see Figure 3c, and at 266 nm, not shown).

**Quantum Yields.** We irradiated solutions of 1.1 mM ONOO<sup>-</sup> in 5 mM KOH (final pH 11.7) as described by Nauser and Koppenol<sup>4</sup> and used eq 7 to calculate the quantum yields ( $\phi$ ) of the reactions:

$$\phi = \frac{c_{\text{products}}}{c_{\text{absorbed photons}}} \quad (7)$$

where  $c_{\text{products}}$  is the concentration of the product; furthermore,  $c_{\text{absorbed photons}} = c_{\text{total photons}} (1 - T)$ , or

$$c_{\text{absorbed photons}} = \frac{E_{\text{pulse}} \times \lambda}{h \times c \times N_A \times V_{\text{irradiated}}} (1 - 10^{-[\text{HOONO}] \times \epsilon \times l_{\text{laser}}}) \quad (8)$$

where  $E_{\text{pulse}}$  is the laser energy,  $\lambda$  is the wavelength of irradiation,  $h$  is the Planck constant,  $c$  is the speed of light,  $N_A$  is Avogadro's number,  $V_{\text{irradiated}}$  is the irradiated sample volume,  $\epsilon$  is the molar absorptivity at the irradiation wavelength, and  $l_{\text{laser}}$  is the laser path length within the cell. The quantum yields were calculated at a delay time of 75 ns. We determined a quantum yield of  $0.18 \pm 0.03$  for the generation of NO• and O<sub>2</sub>•<sup>-</sup> from ONOO<sup>-</sup>. In addition, we found the same quantum yield when we re-evaluated the experimental data in the work of Nauser and Koppenol.<sup>4</sup>

Similarly, we calculated a quantum yield for the induced N–O bond scission of ONOOH of  $0.15 \pm 0.03$  at

355 nm and  $0.18 \pm 0.04$  at 266 nm. The quantum yield of the NO<sub>3</sub><sup>-</sup> excitation to form ONOOH is 0.007.

## Discussion

The main conclusion that we can draw from the work we present here is that laser flash photolysis of ONOOH at 355 nm causes scission of the N–O and not the O–O bond.

**Photolysis of NO<sub>3</sub><sup>-</sup>.** Depending on pH, photolysis of the NO<sub>3</sub><sup>-</sup> solutions leads to the formation of ONOO<sup>-</sup> and ONOOH.<sup>39–44</sup> Upon irradiation of NO<sub>3</sub><sup>-</sup> solutions at 266 nm, we observe an immediate increase in absorbance, followed by a pH-dependent decay with a second-order rate constant of  $(1.7 \pm 0.8) \times 10^{10} \text{ M}^{-1} \text{ s}^{-1}$ , which we ascribe to the protonation of ONOO<sup>-</sup> to form ONOOH, and a subsequent decay of ONOOH ( $k_1 = 1.2 \text{ s}^{-1}$ ).<sup>8</sup> Identical results were obtained for Li<sup>+</sup>, Na<sup>+</sup>, K<sup>+</sup>, and Cs<sup>+</sup> salts of NO<sub>3</sub><sup>-</sup>; RbNO<sub>3</sub> could not be tested because of its low solubility. Photolysis of (Me<sub>4</sub>N)NO<sub>3</sub> solutions yields qualitatively different results, in which we observe an initial absorbance increase instead of a rapid decay that we assume is due to the reaction of (Me<sub>4</sub>N)<sup>+</sup> with products of two-photon processes. It is possible that irradiation of solutions at 266 nm results in a two-photon excitation of H<sub>2</sub>O to generate reactive species such as HO•. Since alkali metal ions, unlike (Me<sub>4</sub>N)<sup>+</sup>, do not react with HO•, we decided to use LiONOO for experiments with ONOOH.

**Photolysis of ONOOH.** At pH 2.1, with excitation at 355 nm, the photolysis of ONOOH triggers a reversible process: We observe an increase in absorbance at 260 nm upon photolysis that is pH-dependent between pH 4.1 and 5.4 (Figure 2B), as well as bleaching at 330 nm, both of which return to preirradiation levels. The increase in absorption at 260 nm could be explained by the formation of either NO<sub>2</sub>• + HO• (reaction 4) or HO<sub>2</sub>• + NO• (reaction 5). However, we favor the reversible formation of HO<sub>2</sub>• and NO• (reaction 5) over reaction 4 as the major pathway, because (i) at 260 nm, we observe a pH-dependent increase in absorbance around pH = 4.8, the pK<sub>a,6</sub> of HO<sub>2</sub>• (Figure 2B),<sup>28</sup> whereas the sum of absorptivities of HO• and NO<sub>2</sub>• is not pH-dependent, as neither NO<sub>2</sub>• nor HO• has a pK<sub>a</sub> in that region at 260 nm; (ii) the bleaching observed at 330–400 nm, rather than the absorption increase expected for reaction 4, may be explained by the formation of HO<sub>2</sub>• and NO• (reaction 5), because the molar absorptivities of HO<sub>2</sub>• and NO• at 330 nm are lower than that of ONOOH (Table 1); (iii) the scavenging experiments with Cl<sup>-</sup> indicate that •OH formation is negligible, and neither HO<sub>2</sub>• nor NO• would oxidize Cl<sup>-</sup>; (iv) any excess ONOOH is expected to be oxidized by •OH but not by HO<sub>2</sub>• or NO•; thus, the relaxation of the absorbance signal for ONOOH to the preirradiation level indicates that no •OH is formed (by contrast, •OH from the radiolysis of water produced by irradiation at 266 nm reacts with excess ONOOH, and

(39) Papée, H. M.; Petriconi, G. L. *Nature* **1964**, *204*, 142–144.

(40) Shuali, U.; Ottolenghi, M.; Rabani, J.; Yelin, S. *J. Phys. Chem.* **1969**, *73*, 3445–3451.

(41) Barat, F.; Gilles, L.; Hickel, B.; Sutton, J. *J. Chem. Soc. A* **1970**, 1982–1986.

(42) Bayliss, N. S.; Bucat, R. B. *Aust. J. Chem.* **1975**, *28*, 1865–1878.

(43) Wagner, I.; Strehlow, H.; Busse, G. *Z. Physik. Chem.* **1980**, *123*, 1–33.

(44) Madsen, D.; Larsen, J.; Jensen, S. K.; Keiding, S. R.; Thøgersen, J. *J. Am. Chem. Soc.* **2003**, *125*, 15571–15576.

relaxation of the absorbance signal to preirradiation levels is not observed); and (v) at both excitation wavelengths, the spectra collected at pH 4.83 fit calculated spectra.

We report here a rate constant  $k_{-5} = (1.2 \pm 0.2) \times 10^{10} \text{ M}^{-1} \text{ s}^{-1}$  for the recombination of  $\text{HO}_2^\bullet$  with  $\text{NO}^\bullet$  at pH 4.1–5.4. This rate constant is ca. 4-fold higher than the value obtained by pulse radiolysis,  $3.2 \times 10^9 \text{ M}^{-1} \text{ s}^{-1}$ ,<sup>29</sup> and equivalent to that observed in basic aqueous solutions for the reaction of  $\text{O}_2^{\bullet-}$  with  $\text{NO}^\bullet$ ,  $(1.6 \pm 0.3) \times 10^{10} \text{ M}^{-1} \text{ s}^{-1}$ .<sup>4</sup> With  $k_{-5} = (1.2 \pm 0.2) \times 10^{10} \text{ M}^{-1} \text{ s}^{-1}$ , we calculate a rate constant  $k_5 = 0.0003 \text{ s}^{-1}$  for the homolysis of ONOOH to  $\text{HO}_2^\bullet$  and  $\text{NO}^\bullet$ . This rate constant indicates that it is not possible to detect this homolysis reaction because ONOOH isomerizes with a rate constant of  $1.2 \text{ s}^{-1}$ .

The results of our investigations of photolysis of  $(\text{Me}_4\text{N})\text{ONOO}$  solutions (Figure 3) were similar to those found with  $\text{LiONOO}$  (Figure 2), probably because the concentration of  $(\text{Me}_4\text{N})\text{ONOO}$  was much lower, 1 mM, than the 1 M solutions used in the  $(\text{Me}_4\text{N})\text{NO}_3$  experiments. The decay in absorbance after photolysis at 266 nm of  $(\text{Me}_4\text{N})\text{ONOO}$  solutions ends at levels lower than the absorbance of the initial mixture (Figure 5), possibly because two-photon processes lead to the formation of products that react either with the remaining ONOOH or with the formed  $\text{HO}_2^\bullet$ ,  $\text{O}_2^{\bullet-}$ , and  $\text{NO}^\bullet$ . We further assume that  $\text{HO}^\bullet$  produced by two-photon excitation of  $\text{H}_2\text{O}$  reacts more rapidly with ONOOH than with  $(\text{Me}_4\text{N})^+$ .

**Quantum Yields.** For all experimental conditions, whether acidic (ONOOH) or basic ( $\text{ONOO}^-$ ), the quantum yields resulting from excitation at 266 or 355 nm are essentially identical (15%) within the error, which allows us to conclude that similar energies are required to break the N–O bond in both  $\text{ONOO}^-$  and ONOOH. The activation energy for homolysis of the N–O bond of  $\text{ONOO}^-$  is  $102 \text{ kJ mol}^{-1}$  and that of  $\text{O}_2\text{NOO}^-$  is  $93 \text{ kJ mol}^{-1}$ ,<sup>9,50</sup> hence, we estimate a N–O bond dissociation energy of  $100 \text{ kJ mol}^{-1}$  for ONOOH. Furthermore, we assume that the remaining 85% of the quantum yield can be assigned to an excited state of ONOOH that rapidly decays to the ground state.

**Formation of  $\text{HO}^\bullet$  by Photolysis.** To detect yields of O–O homolysis, we trapped  $\text{HO}^\bullet$  with  $\text{Cl}^-$ . In contrast to  $\text{Br}^-$  and  $\text{I}^-$ ,  $\text{Cl}^-$  does not react with ONOOH or its decomposition products.<sup>24,51,52</sup> We determined a yield of  $0.9 \mu\text{M HO}^\bullet$  for the homolysis of ONOOH under conditions that produced more than  $25 \mu\text{M HO}_2$  and  $\text{NO}^\bullet$ . In control experiments in which we irradiated acidic  $\text{Cl}^-$  solutions at 355 nm laser light (135 mJ/pulse) in the absence of ONOOH, we observed no formation of  $\text{Cl}_2^{\bullet-}$  at 340 nm. However, with excitation at 266 nm

(108 mJ/pulse), we observed the formation of  $5 \mu\text{M HO}^\bullet$ , which implies that two-photon reactions are relevant at this excitation wavelength.<sup>37</sup> Subsequent reaction of  $\text{HO}^\bullet$  with ONOOH explains the loss of absorbance after the recombination of  $\text{HO}_2^\bullet$  and  $\text{NO}^\bullet$ . We assume that the rate constant for the reaction of  $\text{HO}^\bullet$  with concentrated ONOOH is similar to that for the reaction with the anion,  $(4.8\text{--}5.8) \times 10^9 \text{ M}^{-1} \text{ s}^{-1}$ .<sup>8,53</sup> By implication, then, two-photon excitation of the solvent at 355 nm is irrelevant, and any  $\text{Cl}_2^{\bullet-}$  formed originates from the  $\text{HO}^\bullet$  generated by ONOOH photolysis. The reaction of  $\text{O}_2^{\bullet-}$  with  $\text{Cl}^-$  is negligible, with a rate constant of  $<0.014 \text{ M}^{-1} \text{ s}^{-1}$ .<sup>54</sup> Reactions of  $\text{HO}_2^\bullet$  and  $\text{O}_2^{\bullet-}$  with  $\text{HO}^\bullet$ , which have rate constants of  $(0.7\text{--}1.0) \times 10^{10} \text{ M}^{-1} \text{ s}^{-1}$ ,<sup>55,56</sup> and  $(0.9\text{--}1.0) \times 10^{10} \text{ M}^{-1} \text{ s}^{-1}$ ,<sup>55,56</sup> respectively, and of  $\text{NO}^\bullet$  with  $\text{HO}^\bullet$ , with a rate constant of  $(1.7\text{--}2.0) \times 10^{10} \text{ M}^{-1} \text{ s}^{-1}$ ,<sup>49,57</sup> are also unimportant. Finally, with respect to the reaction of  $\text{NO}^\bullet$  with  $\text{HO}_2^\bullet$ , we can neglect reactions of  $\text{HO}_2^\bullet$  with itself ( $k = 1.0 \times 10^6 \text{ M}^{-1} \text{ s}^{-1}$ )<sup>58</sup> or with  $\text{O}_2^{\bullet-}$  ( $k = 9.7 \times 10^7 \text{ M}^{-1} \text{ s}^{-1}$ ).<sup>28</sup>

Our results obtained by photolysis at 355 nm show that the yields of the photolysis products are  $<5\%$  of  $\text{HO}^\bullet$  and  $\text{NO}_2^\bullet$  in comparison to  $>95\%$  of  $\text{HO}_2^\bullet$  and  $\text{NO}^\bullet$ . These results are counterintuitive within the framework of the given thermodynamic data on ONOOH,  $\text{NO}^\bullet$ ,  $\text{HO}_2^\bullet$ ,  $\text{NO}_2^\bullet$ , and  $\text{HO}^\bullet$  shown in Figure 1 in that, without regard to activation energies, these data favor  $\text{NO}_2^\bullet$  and  $\text{HO}^\bullet$  as homolysis products. An obvious argument is that photochemistry processes involve excited states and reaction pathways different from those that involve ground-state structures.

In a report combining infrared spectroscopy data with quantum calculations, it has been suggested that ONOOH may undergo homolysis, directly and reversibly, to form  $\text{NO}^\bullet$  and  $\text{HO}_2^\bullet$ , and, indirectly, by way of several intermediates to  $\text{NO}_2^\bullet$  and  $\text{HO}^\bullet$ .<sup>59</sup> Additionally, isomerization to  $\text{NO}_3^-$  and  $\text{H}^+$  acts as a sink that effectively prevents the formation of free  $\text{NO}_2^\bullet$  and  $\text{HO}^\bullet$ . If this is so, then how can ONOOH act as a powerful oxidant? According to a recent ab initio study, ONOOH reacts by way of a two-state reactivity paradigm in which the activated and oxidizing form of ONOOH is a triplet-state intermediate described as a “hydroxyl radical stabilized by a nitrogen dioxide group”.<sup>60</sup> The findings of Contreras et al.<sup>60</sup> support our position that isomerization of ONOOH takes place via intramolecular reorganization rather than by homolysis.

**Acknowledgment.** We thank Dr. P. L. Bounds for helpful discussions and linguistic advice. The studies were supported by the ETH Zurich and the Swiss National Science Foundation.

(45) Nielsen, S. O.; Michael, B. D.; Hart, E. J. *J. Phys. Chem.* **1976**, *80*, 2482–2488.

(46) Pagsberg, P.; Christensen, H.; Rabani, J.; Nilsson, G.; Fenger, J.; Nielsen, S. O. *J. Phys. Chem.* **1969**, *73*, 1029–1038.

(47) Czapski, G.; Bielski, B. H. J. *Radiat. Phys. Chem.* **1993**, *41*, 503–505.

(48) Grätzel, M.; Henglein, A.; Lilie, J.; Beck, G. *Ber. Bunsenges. Physik. Chem.* **1969**, *73*, 646–653.

(49) Treinin, A.; Hayon, E. *J. Am. Chem. Soc.* **1970**, *92*, 5821–5828.

(50) Zabel, F. *Z. Physik. Chem.* **1995**, *188*, 119–142.

(51) Halfpenny, E.; Robinson, P. L. *J. Chem. Soc.* **1952**, 928–938.

(52) Goldstein, S.; Czapski, G. *Inorg. Chem.* **1995**, *34*, 4041–4048.

(53) Goldstein, S.; Saha, A.; Lyman, S. V.; Czapski, G. *J. Am. Chem. Soc.* **1998**, *120*, 5549–5554.

(54) Long, C. A.; Bielski, B. H. J. *J. Phys. Chem.* **1980**, *84*, 555–557.

(55) Sehested, K.; Rasmussen, O. L.; Fricke, H. *J. Phys. Chem.* **1968**, *72*, 626–630.

(56) Elliot, A. J.; Buxton, G. V. *J. Chem. Soc., Faraday Trans.* **1992**, *88*, 2465–2470.

(57) Strehlow, H.; Wagner, I. *Z. Phys. Chem.* **1982**, *132*, 151–160.

(58) Christensen, H.; Sehested, K. *J. Phys. Chem.* **1988**, *92*, 3007–3011.

(59) Konen, I. M.; Pollack, I. B.; Li, E. X. J.; Lester, M. I.; Varner, M. E.; Stanton, J. F. *J. Chem. Phys.* **2005**, *122*, 094320–1–094320–16.

(60) Contreras, R.; Galván, M.; Oliva, M.; Safont, V. S.; Andrés, J.; Guerra, D.; Aizman, A. *Chem. Phys. Lett.* **2008**, *457*, 216–221.